Optik - International Journal for Light and Electron Optics 182 (2019) 1204–1210

Contents lists available at ScienceDirect

Optik

journal homepage: www.elsevier.com/locate/ijleo

Original research article

Effect of defect density and energy level mismatch on the performance of perovskite solar cells by numerical simulation

M.S. Jamal[a,b], S.A. Shahahmadi[c,*], Mohd. Aizat Abdul Wadi[a], P. Chelvanathan[a], N. Asim[a], H. Misran[c], M.I. Hossain[e], N. Amin[c,d], K. Sopian[a], Md. Akhtaruzzaman[a,*]

[a] *Solar Energy Research Institute (SERI), Universiti Kebangsaan Malaysia (UKM), 43600 Bangi, Selangor, Malaysia*
[b] *Institute of Fuel Research and Development (IFRD), BCSIR, Dhaka 1205, Bangladesh*
[c] *Institute of Sustainable Energy (ISE), Universiti Tenaga Nasional (@The National Energy University), Jalan IKRAM-UNITEN, 43000 Kajang, Selangor, Malaysia*
[d] *Department of Electrical, Electronics and System Engineering, Universiti Kebangsaan Malaysia (UKM), 43600 Bangi, Selangor, Malaysia*
[e] *Qatar Environment and Energy Research Institute, Hamad Bin Khalifa University, Doha, Qatar*

ARTICLE INFO

Keywords:
Defect density
Defect level
Numerical simulation
Perovskite solar cell
SCAPS-1D

ABSTRACT

The defects at the absorber and interface layer of organic-inorganic lead halide perovskite solar cells are unfavorable for efficiency as well as the stability. In this study, we have performed the numerical simulation on inverted planar structure perovskite solar cell based on NiO as a hole transport material (HTM) by SCAPS^{-1}D. Here we investigated the effects of defect density and energy level of the perovskite absorber layer and perovskite/HTM interface layer on the performance, respectively. The analysis revealed that values of J_{sc}, V_{oc}, and FF of perovskite solar cells are significantly reduced with increasing the defect density of perovskite layer. The power conversion efficiency severely reduced from 25 to 5% when the defect density increased from 10^{13} to $10^{18}\,\text{cm}^{-3}$, respectively. A similar trend was also found in case of interfacial defect between Perovskite and HTM layer. It was found that the defect energy level more than 0.3 eV above conduction band of perovskite has almost no detrimental effect on the device's efficiency.

1. Introduction

Metal halide perovskite solar cells (PSCs) have been identified as the most attractive photovoltaic technology for energy harvesting due to their exceptional semiconducting properties likely long diffusion length (~175 μm) [1], high charge carrier lifetime (> 15μs) [2], large absorption coefficient (> $0.5 \times 10^4\,\text{cm}^{-1}$) [3], high carrier mobility (~$20\,\text{cm}^2\,\text{V}^{-1}\,\text{s}^{-1}$) [4], and tunable bandgap (1.2 up to 2.3 eV) [5]. These properties are encouraging to use in the fabrication of metal halide PSCs. The PSCs are generally engineered with the organic cation-based perovskite compounds as the absorber. Although the initial involvement of perovskite compounds in solar cells showed limited power conversion efficiency (PCE) of less than 4% [6], the rapid chronological development is seen in the shortest period in the solar cell's history. Currently, the record PCE is 22.1% [7] although, long-term stability and current-voltage hysteresis have remained crucial for future development [8]. Theoretically, it is reported that the PCE limit of the PSC (without the angular restriction) is about 31%, which is close to the Shockley-Queisser limit (33%) [9]. However, by using first-principles calculations and thermodynamic modelling, Granas et al. gave the range of bandgaps of the metal-halide-perovskites and stated that the theoretical maximum PCE limit is in the range of ~25–27% [10]. It is expected that this ideal efficiency would be

---

* Corresponding authors.
E-mail addresses: seyedahmad@uniten.edu.my (S.A. Shahahmadi), akhtar.brces@gmail.com (Md. Akhtaruzzaman).

https://doi.org/10.1016/j.ijleo.2018.12.163
Received 15 December 2018; Accepted 27 December 2018

reachable by the usage of high-quality materials, which are defect deficient and optimized in the device structure. In fact, an interface between layers is the most challenging issue, which mainly effect on the stability of the device.

Despite the rapid development in the PSC, its performance has got a considerable margin from aforesaid theoretical limit. High quality perovskite absorber layer with low defect density and less non-radiative recombination process as key factors for further improvement of the PCE should be studied. Understanding of defect formation in absorption layer as well as interlayers are crucial for successful development of stable and highly efficient PSCs. Phase composition for electronic state in perovskite precursor plays an important role on the defect formation and degradation in the stability of PSCs [11]. Fabrication of PSCs are mainly based on solution process that generate a lot of defects such as deep level defect and shallow level defect. These defects reduce the efficiency and reproducibility of PSCs. Although the shallow level defects have been reduced by modifying the deposition methods that led to improve the efficiency and reproducibility of PSCs however, deep level defects of absorption layer and their functions are still under investigation [12]. The performances of PSCs are reduced with increasing defect state density while their effects would be negligible when defect state density is lower than 10^{16} cm^3. Open circuit voltage (V_{oc}) and diffusion length of PSCs are highly affected by Schottky and Frenkel defects [13]. Kim et al. studied the role of intrinsic defects of perovskite materials on photovoltaic properties by density-functional studies. They reported that Schottky defects deal with perovskite precursor solution and do not make any trap state within the bandgap that led to reduce carrier lifetime. Frenkel defects deal with elemental defects vacancies, which explains the accidental doping of perovskite [14].

From the experimental point of view, Ng et al. demonstrated a growth of perovskite layer in ambient by hybrid chemical vapor deposition (HCVD) and they found that the degree of crystallization in perovskite has a strong impact on the defect density. They also disclosed that the HCVD process with slow post deposition cooling rate can significantly reduce the density of shallow and deep traps in the absorber layer [15]. Chouhan et at. reported that defect density at hole transporting layer (HTL)/perovskite interface has strong impact on the V_{oc}, while defect density in the perovskite and perovskite/electron transporting layer (ETL) interface has a major impact on short circuit current density (J_{sc}) [16]. The effect of defect on reaction of HTL surface with perovskite precursor solution was reported by Kim et al. Kim where significant changes in both morphology and atomistic structures at the interface were observed when a native grown NiO on Ni (110) immersed in water and perovskite precursor solution. [17].

In general, based on the obtained review about defects' mechanism in PSCs, we found that the literature is relatively limited. Defects change the optoelectrical properties of a material system and the experimental study about a correlation between defects and optoelectrical properties has lots of challenges apart from the need of exceedingly sophisticated equipment, which is not accessible in many groups. This issue causes undeveloped modeling and, in consequence, defects are disregarded in majority of reported simulations. Although many scientists accept variations in optoelectrical properties while defects are constant with certain values. However, understanding about individual defects' mechanism in simulation software with a constant optoelectrical properties has not been revealed yet. In this work, we have studied the effect of both defect density and energy level in at conduction band of perovskite absorber and HTL interface layers by numerical simulation. Here we simulated the change of efficiency (η), J_{sc}, V_{oc}, and fill factor (FF) by solar cell capacitance simulator (SCAPS^{-1}D) simulation.

2. Methodology

Three types of PSCs have been explored till date include mesoporous, planar, and inverted planar architectures. In this study, the inverted planar architecture ITO/NiO_x/Perovskite/PCBM/Ag is chosen as Fig. 1 depicts in addition of its energy level diagram. As shown, the perovskite active layer is sandwiched between HTL (NiO) and ETL ($PC_{61}BM$) whereas the indium doped tin oxide (ITO) and silver (Ag) are used as a transparent front contact and top metal back contact, correspondingly. Compared with planar and mesoporous PSCs, inverted planar devices exhibits higher stability by eluding the presence of low work function metal cathode and hygroscopic hole-transporting along with vertical phase separation and concentration gradient in perovskite layer [18,19]. Meng et al reported that the inverted planar PSC would exceed efficiency over 18% at lower processing temperature in flexibility with

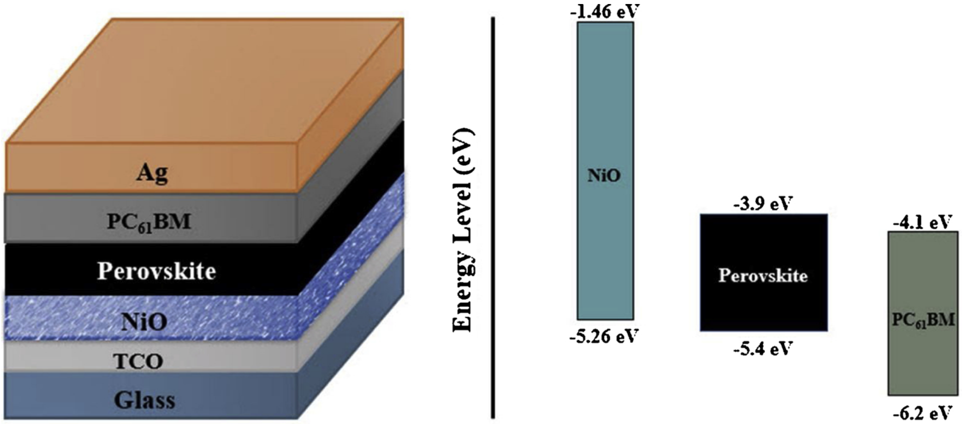

Fig. 1. Schematic presentation of device structure and energy level diagram.

Table 1
List of parameters used in this numerical simulation.

Parameters and units	NiO	Interface	$CH_3NH_3PbI_3$	$PC_{61}BM$
Thickness	50	–	600	80
Bandgap (eV)	3.8 [21]		1.5 [22]	2.1
Electron Affinity (eV)	1.46 [23]		3.9 [24]	4.1
Dielectric Permittivity (relative)	10.7 [25]		10 [26]	4
Effective Conduction Band Density (cm^{-3})	2.8×10^{19} [27]		2.75×10^{18} [28]	2.5×10^{19}
Effective Valence Band Density (cm^{-3})	1.0×10^{19} [27]		3.9×10^{18} [28]	2.5×10^{19}
Electron and Hole thermal velocity (cm/s)	10^7		10^7	10^7
Electron Mobility (cm^2/V.S)	12 [29]		10 [30]	0.01
Hole Mobility (cm^2/V.S)	2.8 [31]		10 [30]	0.01
Acceptor Concentration (cm^{-3})	0 [32]		1×10^9 [32]	0
Donor Concentration (cm^{-3})	1.0×10^{18} [32]		1×10^9 [32]	5×10^{17}
Absorption Interpolation Model	Power law 1		[33]	Power law 1
Radiative recombination coefficient (cm^3/s)	2.3×10^{-9}	3×10^{-11}	3×10^{-11}	2.3×10^{-9}
Auger electron capture coefficient (cm^6/s)	0	0	0	0
Auger hole capture coefficient (cm^6/s)	0	0	0	0
Capture Cross Section for Electrons and Holes (cm^2)	–	10^{-19}	10^{-15}	–
Gaussian defect Energy Level Based on VB (eV)	–	−0.8 - 0.8	−0.9 - -0.1	–
Characteristic Energy (eV)	–	0.1	0.1	–
Defect Density	–	10^{13}-10^{19}	10^{13}-10^{19}	–

insignificant J–V hysteresis [20]. The simulation parameters are summarized from different reported works and displayed in Table 1. The parameters are selected based on available literature to ensure that the obtained outcome from the simulation baseline is the proper reflection of real-world scenario.

The experimentally reported bandgap of perovskite is about 1.5 eV [22]. The electronic band structure of perovskite reveals that the bandgap of perovskite material increases with increasing the electronegativity of metal–site and halide-sites, and the decrease of crystal structures' symmetry (orthorhombic > tetragonal > cubic). Though, there is no general trend to explain the change in bandgap with the variation of organic cation [34]. Electron affinity (χ) is measured experimentally for $CH_3NH_3PbI_3$ about 3.9 eV [35], which is considered for this simulation. For $CH_3NH_3PbI_xCl_{1-x}$ and $CH_3NH_3PbBr_3$, this values are 3.7 ± 1 eV and 3.6 ± 1 eV, respectively [24]. Relative dielectric permittivity (εr) is the ratio of permittivity of the substance to the permittivity of vacuum. εr of perovskites has not yet been played important role for good performance, but it is widely used to perceive the change possibility on the performance of conventional semiconductor [35]. A wide range (from 6.5 to 60.9) [36,37] of εr values are found for perovskite depending on different experimental outcome. Over the low frequencies, εr is consistent and the value is 60.9 within the range 20 Hz to 1 MHz. It is noteworthy that the ionic component is dropped out at infrared frequencies and fail to electric response that lead to reduce the εr of perovskite where the value is 6.5. Literature review reveals that the charge carrier mobility of organo-lead halide perovskite depends on doping level and the phase of the material. The hole mobility of perovskite ranges from 5-12 cm^2/Vs and electron mobility ranges from 2.5 to 10 cm^2/Vs. In addition, charge carrier mobility is also affected by halogen doping [38]. Literature review also divulges that the hole mobility perovskite increases from lead to tin and decreases from iodide to bromide-based perovskites [39]. Wehrenfennig et al reported that the carrier diffusion length of single halide perovskite exceeds 1 μm and substantially longer for mixed halide perovskite due to the combination of low bi-molecular recombination and high charge mobility [30]. The PCE of PSCs is strongly dependent on the thickness of the perovskite film. Improvements in the PCE with increasing the thickness are due to increasing the shunt resistance and optical density [40]. With all that being said, various parameters of perovskite materials change the value PCE, Jsc, Voc and FF of the device. All optimum parameters of perovskite materials have been used in this simulation.

3. Results and discussions

In PSCs, the perovskite absorber layer absorbs photons from sunlight where the photons energy is larger than the bandgap of absorber layer that generates excitons. These excitons are basically negatively charged electron and positively charged hole pairs. These electron and hole diffuse to both sides of the absorber layer and facilitated by additional ETL in one side and HTL at other side. In an efficient PSC, electrons are attracted by ETL and simultaneously holes are repelled. Similarly, HTM attracts the holes from the excitons leaving free electrons. These free electrons must be successfully extracted by the ETM. Electrons are transported to the cathode through ETM and holes are transported to the anode by HTM. This subsequent motion of the electrons and holes generates electrical current. Except this basic principle, some unavoidable defects densities are found in solar cell materials that lead to reduce the overall performance of PSCs. PCE can improve by changing the band offset of electron and hole transporting layer but couldn't achieve the maximum theoretical conversion efficiency. To achieve the maximum PCE, it is necessary to understand the effect of defect density on the performance of perovskite solar cell.

3.1. Effect of absorber layer defect on the PV parameters of PSCs

The performance of PSCs is subjected of two key processes. One is a generation of charge carriers and another is a recombination. When sunlight is incident on PSCs, photo-generated carriers (electron and holes) are generated on the absorber layer. These photo-generated carriers are subsequently collected by the electrode and transfer towards the external current. During the collection of photo-generated charge carriers, a large number of carriers is lost due to the poor quality of perovskite layer. Higher defect density causes higher recombination rate in the low-quality perovskite films that leads to reduce the diffusion length of charge carriers as well as the life time of carriers. Shockley-Read-Hall (SRH) recombination could explain the possible recombination mechanisms to determine the effect of defect density on the performance of PSCs, they are given in Eq. 1 [41].

$$\mathfrak{R}^{SRH} = \frac{\vartheta \sigma_n \sigma_p N_T [np - n_i^2]}{\sigma_p [p + p_1] + \sigma_n [n + n_1]} \tag{1}$$

Where σ_n *and* σ_p are capture cross-sections for electrons and holes, ϑ is electron thermal velocity, N_T number of defects per volume, n_i intrinsic number density, n & p are the concentrations of electron and hole at equilibrium and n_1 and p_1 are the concentrations of electrons and holes in trap defect and valance band, respectively. According to equation 1, $\mathfrak{R}^{SRH}$ is directly proportional to the defect density of perovskite absorber layer. Carrier diffusion length is considered to analyze the effect of defect density on the performance of device depending on SRH effect and diffusion length formula. Haider et al. reported that the diffusion length increases with decreasing the defect density of perovskite absorber layer. This phenomenon leads towards the better performance of perovskite solar cell [13]. The relation between the diffusion length and the carrier mobility and lifetime is expressed in Eq. 2 [42].

$$\boldsymbol{L_D} = \sqrt{\frac{\mu_{(e,h)} \mathfrak{R} T}{q} \tau_{lifetime}} \tag{2}$$

Here, L_D, μ(e,h), and $\tau_{lifetime}$ is the diffusion length, the electron and hole mobility, and the minority-carrier lifetime, respectively. Meanwhile, $\tau_{lifetime}$ depends upon the defect trap density and capture cross-section area for electrons and holes. The relation between $\tau_{lifetime}$ and bulk defect density is expressed in Eq. 3[42].

$$\tau_{lifetime} = \frac{1}{N_t \delta \upsilon_{th}} \tag{3}$$

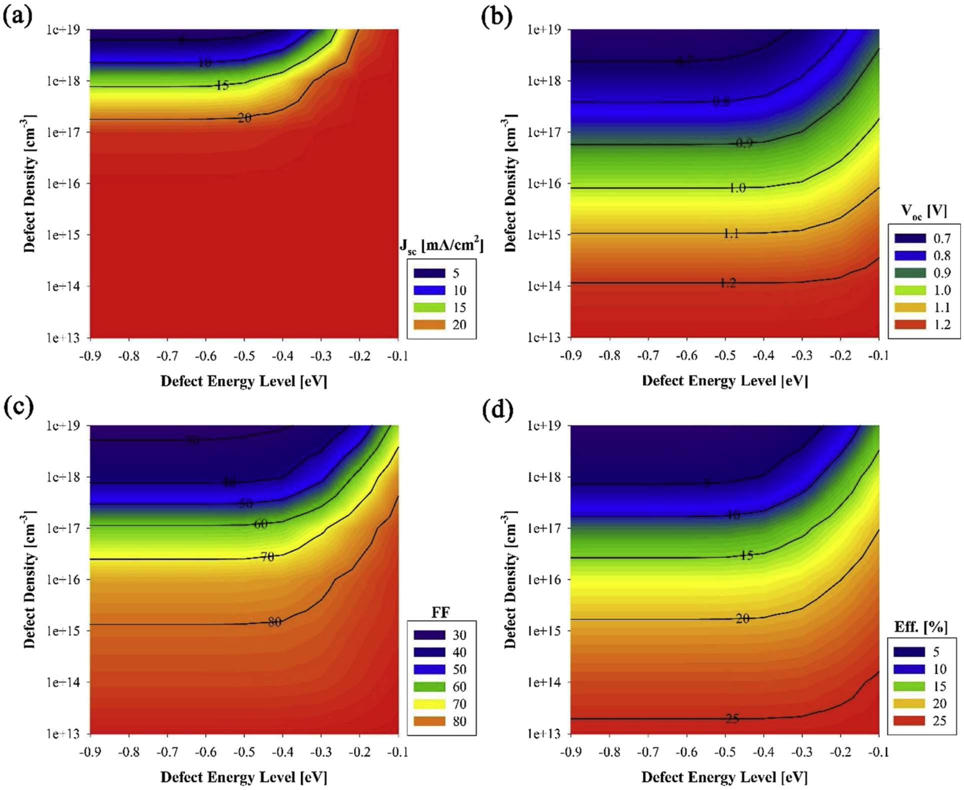

Fig. 2. Contour graphs of perovskite solar cell performance parameters dependency on of absorber defect density and defect energy level (perovskite's conduction band is chosen as the reference) variables.

Here, δ, $\upsilon_{th,}$ and N_t represents the capture cross-section area for electrons and holes, thermal velocity of carriers, and defect density respectively. Fig. 2 represents contour graphs of PSCs photovoltaic characteristics dependency on absorber defect density and defect energy level variables. The effect of defect density ranges (10^{13} to $10^{19}\,cm^{-3}$) and defect energy level (-0.9 to -0.1 eV) is probed based on the conduction band as the reference, while keeping all other parameters constant to explore the device performance. In accordance with presented equations, as shown in Fig. 2 (a), the J_{sc} value reduces significantly with defect density of perovskite layer. The J_{sc} sharply reduces from 20 to 5 mA/cm^2 when defect density of perovskite absorber layer increases from 10^{17} to 10^{19} cm^{-3}. There is no effect in J_{sc} as the defect density is $< 10^{17}$ cm^{-3} even though the defect energy level varied from -0.9 to -0.1 eV. The V_{oc} reduces substantially from 1.2 to 0.7 V when the defect density increases from 10^{14} to 10^{19} cm^{-3} as shown in Fig. 2(b). It is also quite evident that the values of V_{oc} are languidly varied with the defect energy level.

Soucase et al. reported that the V_{oc} is highly influenced by the defect of absorber layer [41]. From practical point of view, the defect densities of perovskite depend on the formation energy, and subsequently chemical potential. It corresponds to precursors, partial pressure, and temperature during synthesis. The defects with low formation energy create only shallow level, which results the long electron-hole diffusion length and high V_{oc}. On the other hand defects with deep levels have high formation energy that results into unpleasant effect on electron-hole diffusion length and V_{oc}. Experimental and simulation results of the long electron-hole diffusion length and high V_{oc} conforms the unusual shallow defect level [43]. Fig. 1(c) reveals that the FF dramatically decreases from 80 to 30% when the defect density increases from 10^{15} to 10^{19} cm^{-3}. However, the FF gradually increases with increasing the defect energy level. Ideally, FF is a function of the V_{oc}, although practically FF is not only dependent on V_{oc} but also the dependent on recombination process of depletion region. Finally, as shown in Fig. 2 (d), we found a predictable trend in the PCE as a result of J_{sc}, V_{oc}, and FF. The PCE drastically reduces from 25 to 5% when the defect densities increase from 10^{13} to $10^{18}\,cm^{-3}$ but the PCE is linearly increases with increasing the defect energy level.

3.2. Effect of defect density of Perovskite/NiO interface layer on the PV parameters of PSCs

Structural mismatch of two different materials leads to initiate the interfacial defects, which cause the charge recombination in the PSCs. Fig. 3 demonstrates the effect of interfacial defect density of HTM/Perovskite layer on the device performance. As shown, the interface quality of HTM/Perovskite layer has a significant impact on solar cell performance. Both defect density (10^{13}-$10^{19}\,cm^{-3}$) and defect energy level (-0.8 to +0.8 eV in which the perovskite's conduction band is chosen as the reference) are investigated. Fig. 3(a) shows the dependency of Jsc on the defect density and energy level. As shown, the Jsc value changes insignificantly from 23.2 to 22.0 mA/cm^2 when the defect density of interface layer increases from 10^{16} to $10^{19}\,cm^{-3}$. No changes are found at the defect density $< 10^{16}$ cm^{-3} even though the defect energy level varied from -0.8 to +0.8 eV.

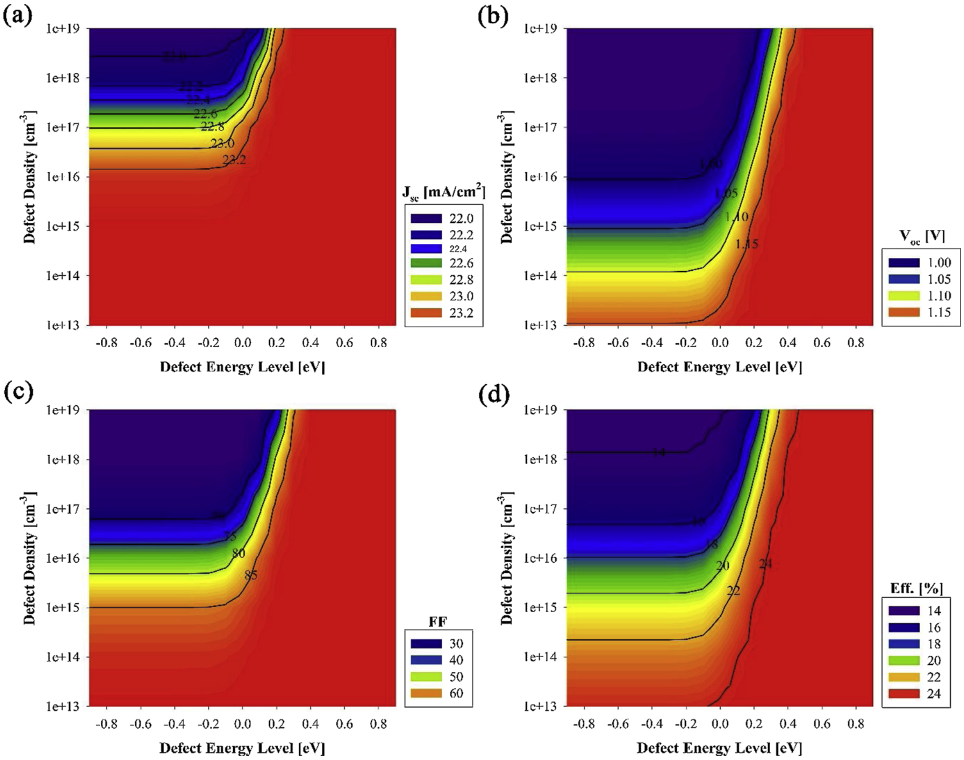

Fig. 3. Contour graphs of perovskite solar cell performance parameters dependency on of interface defect density and defect energy level (perovskite's conduction band is chosen as the reference) variables.

In Fig. 3(b), the values of V_{oc} reduce substantially from 1.15 to 1.00 V while the defect density increases from 10^{13} to 10^{16} cm^{-3}. At defect density > 10^{16} cm^{-3}, there is no change in $V_{oc.}$ It is also quite evident that the major changes in V_{oc} vary from 1.00 to 1.15 V due to the defect energy level existed between 0.2 to 0.4 eV. Fig. 1(c) reveals that the FF decreases from 60 to 30% when the defect density increases from 10^{15} to 10^{17} cm^{-3}. However, beyond this range, there is no effect of defect density on the FF. The FF dramatically changes and becomes twice when the defect energy level increases from 0.1 to 0.3 eV. Fig. 3(d) unveils that defect density of HTM/Perovskite interface layer has a significant effect on the PCE of PSCs. The PCE reduces from 24 to 14% when the defect densities increase from 10^{13} to 10^{19} cm^{-3} but the PCE is linearly increases with increasing the defect energy level ranging from 0.0 to 0.5 eV of perovskite absorber layer. No effect on PCE at higher defect energy level (higher than 0.4 eV). Rate of recombination increases with increasing the defect density of interface layer that lead to reduce the PCE of PSCs.

4. Conclusion

Numerical simulation of inverted planar perovskite solar cell having the architecture ITO/NiO/Perovskite/PCBM/Ag was designed and the effect of defect state of perovskite absorber layer and perovskite/HTM interface layer was investigated. Defect density and defect level of perovskite absorber layer and perovskite/HTM interface layer at the conduction band showed a significant decline of performance. At the perovskite's conduction band, various values of defect density (10^{13} to 10^{19} cm^{-3}) were studied at different energy level up to -0.9 eV. It was found that a deeper defect energy level (< 0.2 eV) as well as a higher defect density would result in a low device efficiency from 25 to 5%. On the other hand, results from interface showed that the defect mechanism had lesser influence on device performance compared with absorber layer since the efficiency dropped from 24 to 14% in overall. It was found that the defect energy level lesser than 0.3 eV above conduction band of perovskite up to -0.8 eV deep inside perovskite has the most detrimental effects.

Based on this study, we have shown that the correlation between device performance and both defect density and energy level is almost linear in simulation, if the optoelectrical properties were chosen constantly. From experimental point of view, defects are the main contributors for optoelectrical changes. In fact, any changes in optoelectrical properties (which are studied in majorities of the literature) should be initiated from defect mechanism and have to be derived from their unique defect properties. This correlation is a challengeable work, which has not been satisfied by scientists yet. Therefore, although keeping constant parameters for defects in simulation would leave a margin between simulation and experimental results, however, the general trend towards the favorable range in device's performance might not be affected.

Acknowledgements

The authors would like to acknowledge Universiti Kebangsaan Malaysia through its Fundamental Research Grant Scheme (FRGS) with code FRGS/1/2017/TK07/UKM/ 02/9. Due appreciation is also credited to the Institute of Sustainable Energy (ISE) of the Universiti Tenaga Nasional (@The National Energy University) for their cordial support through BOLD2025 Program.

References

[1] Q. Dong, Y. Fang, Y. Shao, P. Mulligan, J. Qiu, L. Cao, J. Huang, Electron-hole diffusion lengths& 175 μm in solution grown CH3NH3PbI3 single crystals, Science (2015) aaa5760.

[2] Y. Bi, E.M. Hutter, Y. Fang, Q. Dong, J. Huang, T.J. Savenije, Charge carrier lifetimes exceeding 15 μs in methylammonium lead iodide single crystals, J. Phys. Chem. Lett. 7 (2016) 923–928.

[3] N.-G. Park, Perovskite solar cells: an emerging photovoltaic technology, Mater. Today 18 (2015) 65–72.

[4] H. Oga, A. Saeki, Y. Ogomi, S. Hayase, S. Seki, Improved understanding of the electronic and energetic landscapes of perovskite solar cells: high local charge carrier mobility, reduced recombination, and extremely shallow traps, J. Am. Chem. Soc. 136 (2014) 13818–13825.

[5] T.C.-J. Yang, P. Fiala, Q. Jeangros, C. Ballif, High-bandgap perovskite materials for multijunction solar cells, Joule (2018).

[6] A. Kojima, K. Teshima, Y. Shirai, T. Miyasaka, Organometal halide perovskites as visible-light sensitizers for photovoltaic cells, J. Am. Chem. Soc. 131 (2009) 6050–6051.

[7] W.S. Yang, B.-W. Park, E.H. Jung, N.J. Jeon, Y.C. Kim, D.U. Lee, S.S. Shin, J. Seo, E.K. Kim, J.H. Noh, Iodide management in formamidinium-lead-halide–based perovskite layers for efficient solar cells, Science 356 (2017) 1376–1379.

[8] J. Burschka, N. Pellet, S.-J. Moon, R. Humphry-Baker, P. Gao, M.K. Nazeeruddin, M. Grätzel, Sequential deposition as a route to high-performance perovskite-sensitized solar cells, Nature 499 (2013) 316.

[9] W.E. Sha, X. Ren, L. Chen, W.C. Choy, The efficiency limit of CH3NH3PbI3 perovskite solar cells, Appl. Phys. Lett. 106 (2015) 221104.

[10] O. Grånäs, D. Vinichenko, E. Kaxiras, Establishing the limits of efficiency of perovskite solar cells from first principles modeling, Sci. Rep. 6 (2016) 36108.

[11] A. Naikaew, P. Prajongtat, M.C. Lux-Steiner, M. Arunchaiya, T. Dittrich, Role of phase composition for electronic states in CH3NH3PbI3 prepared from CH3NH3I/PbCl2 solution, Appl. Phys. Lett. 106 (2015) 232104.

[12] S. Heo, G. Seo, Y. Lee, D. Lee, M. Seol, J. Lee, J.-B. Park, K. Kim, D.-J. Yun, Y.S. Kim, Deep level trapped defect analysis in CH 3 NH 3 PbI 3 perovskite solar cells by deep level transient spectroscopy, Energy Environ. Sci. 10 (2017) 1128–1133.

[13] S.Z. Haider, H. Anwar, M. Wang, A comprehensive device modelling of perovskite solar cell with inorganic copper iodide as hole transport material, Semicond. Sci. Technol. 33 (2018) 035001.

[14] J. Kim, S.-H. Lee, J.H. Lee, K.-H. Hong, The role of intrinsic defects in methylammonium lead iodide perovskite, J. Phys. Chem. Lett. 5 (2014) 1312–1317.

[15] A. Ng, Z. Ren, Q. Shen, S.H. Cheung, H.C. Gokkaya, S.K. So, A.B. Djurišić, Y. Wan, X. Wu, C. Surya, Crystal engineering for low defect density and high efficiency hybrid chemical vapor deposition grown perovskite solar cells, ACS Appl. Mater. Interfaces 8 (2016) 32805–32814.

[16] A.S. Chouhan, N.P. Jasti, S. Avasthi, Effect of interface defect density on performance of perovskite solar cell: correlation of simulation and experiment, Mater. Lett. (2018).

[17] J. Kim, B. Hou, C. Park, C.B. Bahn, J. Hoffman, J. Black, A. Bhattacharya, N. Balke, H. Hong, J.H. Kim, Effect of defects on reaction of NiO surface with Pb-contained solution, Sci. Rep. 7 (2017) 44805.

[18] C.-H. Hsieh, Y.-J. Cheng, P.-J. Li, C.-H. Chen, M. Dubosc, R.-M. Liang, C.-S. Hsu, Highly efficient and stable inverted polymer solar cells integrated with a cross-linked fullerene material as an interlayer, J. Am. Chem. Soc. 132 (2010) 4887–4893.

[19] Z. Xu, L.M. Chen, G. Yang, C.H. Huang, J. Hou, Y. Wu, G. Li, C.S. Hsu, Y. Yang, Vertical phase separation in Poly (3-hexylthiophene): fullerene derivative blends and its advantage for inverted structure solar cells, Adv. Funct. Mater. 19 (2009) 1227–1234.

[20] L. Meng, J. You, T.-F. Guo, Y. Yang, Recent advances in the inverted planar structure of perovskite solar cells, Acc. Chem. Res. 49 (2015) 155–165.

[21] A.S. Subbiah, A. Halder, S. Ghosh, N. Mahuli, G. Hodes, S.K. Sarkar, Inorganic hole conducting layers for perovskite-based solar cells, J. Phys. Chem. Lett. 5 (2014) 1748–1753.

[22] J. Jeng, Y. Chiang, M. Lee, S. Peng, T. Guo, F. Chen, T. Wen, Methylammonium lead iodide perovskite/fullerene-based hybrid solar cells, SPIE Newsroom 10 (2014) 005033.

[23] H. Wu, L.-S. Wang, A study of nickel monoxide (NiO), nickel dioxide (ONiO), and Ni (O 2) complex by anion photoelectron spectroscopy, J. Chem. Phys. 107 (1997) 16–21.

[24] P. Schulz, E. Edri, S. Kirmayer, G. Hodes, D. Cahen, A. Kahn, Interface energetics in organo-metal halide perovskite-based photovoltaic cells, Energy Environ. Sci. 7 (2014) 1377–1381.

[25] F. Kurnia, H. Hadiyawarman, C. Jung, C. Liu, S. Lee, S. Yang, H. Park, S. Song, C. Hwang, Effect of NiO growth conditions on the bipolar resistance memory switching of Pt/NiO/SRO structure, J. Korean Phys. Soc. 57 (2010) 1856–1861.

[26] C. Homes, T. Vogt, S. Shapiro, S. Wakimoto, A. Ramirez, Optical response of high-dielectric-constant perovskite-related oxide, Science 293 (2001) 673–676.

[27] S. Fonash, Solar Cell Device Physics, Elsevier, 2012.

[28] G. Giorgi, J.-I. Fujisawa, H. Segawa, K. Yamashita, Small photocarrier effective masses featuring ambipolar transport in methylammonium lead iodide perovskite: a density functional analysis, J. Phys. Chem. Lett. 4 (2013) 4213–4216.

[29] W. Chia-Ching, Y. Cheng-Fu, Investigation of the properties of nanostructured Li-doped NiO films using the modified spray pyrolysis method, Nanoscale Res. Lett. 8 (2013) 33.

[30] C. Wehrenfennig, G.E. Eperon, M.B. Johnston, H.J. Snaith, L.M. Herz, High charge carrier mobilities and lifetimes in organolead trihalide perovskites, Adv. Mater. 26 (2014) 1584–1589.

[31] M. Tyagi, M. Tomar, V. Gupta, Influence of hole mobility on the response characteristics of p-type nickel oxide thin film based glucose biosensor, Anal. Chim. Acta 726 (2012) 93–101.

[32] M.I. Hossain, F.H. Alharbi, N. Tabet, Copper oxide as inorganic hole transport material for lead halide perovskite based solar cells, Sol. Energy 120 (2015) 370–380.

[33] Y. Wu, F. Xie, H. Chen, X. Yang, H. Su, M. Cai, Z. Zhou, T. Noda, L. Han, Thermally stable MAPbI3 perovskite solar cells with efficiency of 19.19% and area over 1 cm2 achieved by additive engineering, Adv. Mater. 29 (2017).

[34] S.X. Tao, X. Cao, P.A. Bobbert, Accurate and efficient band gap predictions of metal halide perovskites using the DFT-1/2 method: GW accuracy with DFT expense, Sci. Rep. 7 (2017) 14386.

[35] M.A. Green, A. Ho-Baillie, H.J. Snaith, The emergence of perovskite solar cells, Nat. Photonics 8 (2014) nphoton. 2014.2134.

[36] M. Hirasawa, T. Ishihara, T. Goto, K. Uchida, N. Miura, Magnetoabsorption of the lowest exciton in perovskite-type compound (CH3NH3) PbI3, Physica B Condens. Matter 201 (1994) 427–430.

[37] N. Onoda-Yamamuro, T. Matsuo, H. Suga, Dielectric study of CH3NH3PbX3 (X= Cl, Br, I), J. Phys. Chem. Solids 53 (1992) 935–939.

[38] C. Motta, F. El-Mellouhi, S. Sanvito, Charge carrier mobility in hybrid halide perovskites, Sci. Rep. 5 (2015) 12746.

[39] L.M. Herz, Charge-carrier mobilities in metal halide perovskites: fundamental mechanisms and limits, ACS Energy Lett. 2 (2017) 1539–1548.

[40] D. Liu, M.K. Gangishetty, T.L. Kelly, Effect of CH 3 NH 3 PbI 3 thickness on device efficiency in planar heterojunction perovskite solar cells, J. Mater. Chem. A 2 (2014) 19873–19881.

[41] B.M. Soucase, I.G. Pradas, K.R. Adhikari, Numerical simulations on perovskite photovoltaic devices, Perovskite Materials-Synthesis, Characterisation, Properties, and Applications, InTech, 2016.

[42] M.A. Green, Solar Cells: Operating Principles, Technology, and System Applications, Prentice-Hall, Inc., Englewood Cliffs, NJ, 1982, p. 288.

[43] W.-J. Yin, J.-H. Yang, J. Kang, Y. Yan, S.-H. Wei, Halide perovskite materials for solar cells: a theoretical review, J. Mater. Chem. A 3 (2015) 8926–8942.